Electronic Supplementary Material (ESI) for Nanoscale.

Supporting Information
Macroscopic and Tunable Nanoparticle Superlattices

Honghu Zhang,Wenjie Wang, Surya Mallapragada, Alex Travesset, and David Vaknin
Ames Laboratory, Iowa State University, Ames,Iowa 50011, USA

Control experiments

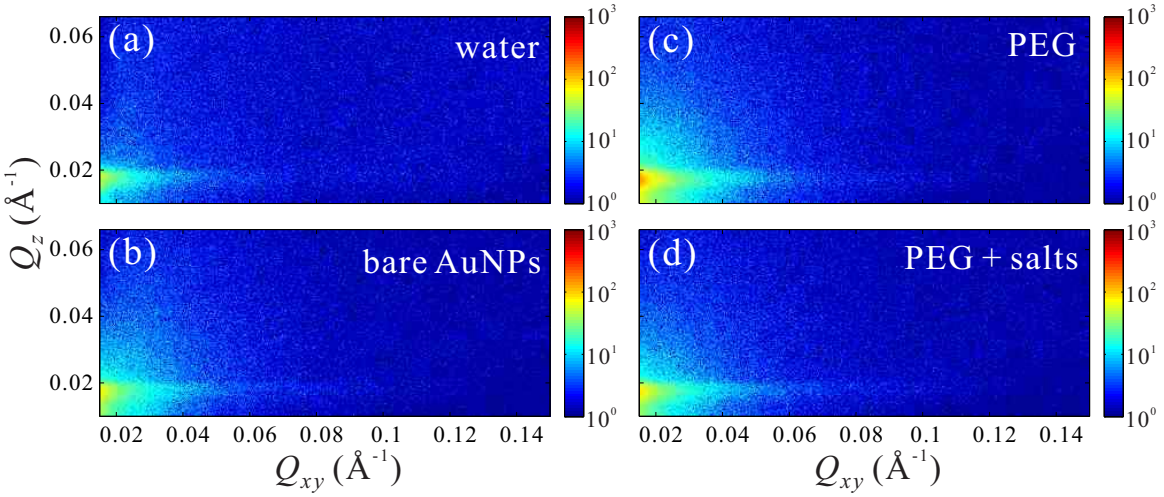

Fig. S1 GISAXS patterns as functions of Q_{xy} and Q_z for (a) pure Millipore water, (b) aqueous solution of 10 nM bare AuNPs prior to PEG functionalization, (c) aqueous solution of 10 μM PEG_{6k}-SH with no salts and (d) PEG_{6k}-SH in 500 mM K_2CO_3. Intensities are displayed on logarithmic scales

Figure S1 (a-d) shows a few GISAXS patterns from various solutions as control experiments to demonstrate the importance of functionalizing the AuNPs with PEG and the effect of salt on the formation of superlattice structures. None of the patterns indicate surface enrichment.

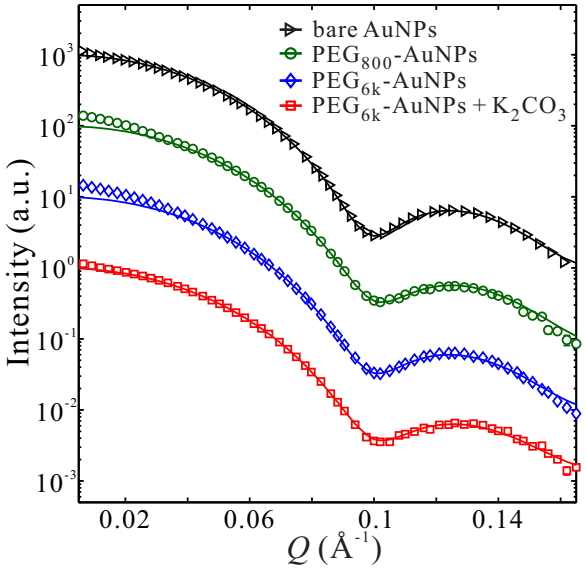

Fig. S2 SAXS intensity profiles of aqueous suspension of unfunctionalized (bare) AuNPs (black triangles), PEG_{800}-AuNPs without salts (green circles), PEG_{6k}-AuNPs without salts (blue diamonds) and PEG_{6k}-AuNPs mixed with 500 mM K_2CO_3 (red squares). The solid lines are best fits using a form factor of spherical particles with polydispersity described by a Gaussian distribution. The size distributions of nanoparticles estimated by the best fits are $D = 8.9 \pm 0.8$ nm (bare AuNPs), 8.7 ± 0.9 nm (PEG_{800}-AuNPs), 8.8 ± 0.9 nm (PEG_{6k}-AuNPs), and 8.7 ± 0.9 nm (PEG_{6k}-AuNPs with salts). These results show that the SAXS patterns are insensitive to the PEG shell around a AuNP (i.e., the corona) indicating that the electron density of the PEG corona in water solution is very close to that of pure water. The curves are vertically shifted for clarity.

Figure S2 shows SAXS measurements of PEG-AuNPs and unfunctionalized (bare) AuNPs dispersed in solution (conducted at Sector 12ID-B at the Advanced Photon Source). The analysis of the measured form factors determines the size and size-distribution of the

AuNPs. These results demonstrate that the form factor is dominated by Au cores regardless of functionalization as the corona formed by PEG around the AuNP has practically the same electron density as that of the water solution (the SAXS data in Fig. S2 are obtained after subtraction of the SAXS of the solvent). This is crucial to the analysis of the X-ray reflectivity analysis given in the main manuscript that shows the ED of the film is dominated by the AuNPs and the submerged corona is practically indistinguishable from the solution.

Superlattice dependence on PEG_{6k}-AuNPs concentrations

In the main manuscript we show the tunability of the hexagonal superlattice by varying salt concentration. Figure S3 shows the GISAXS patterns from various concentrations of PEG_{6k}-AuNPs at a fixed 0.5 M of K_2CO_3. Our theoretical model shows a dependence of the lattice constant that is logarithmic in the AuNPs concentration.

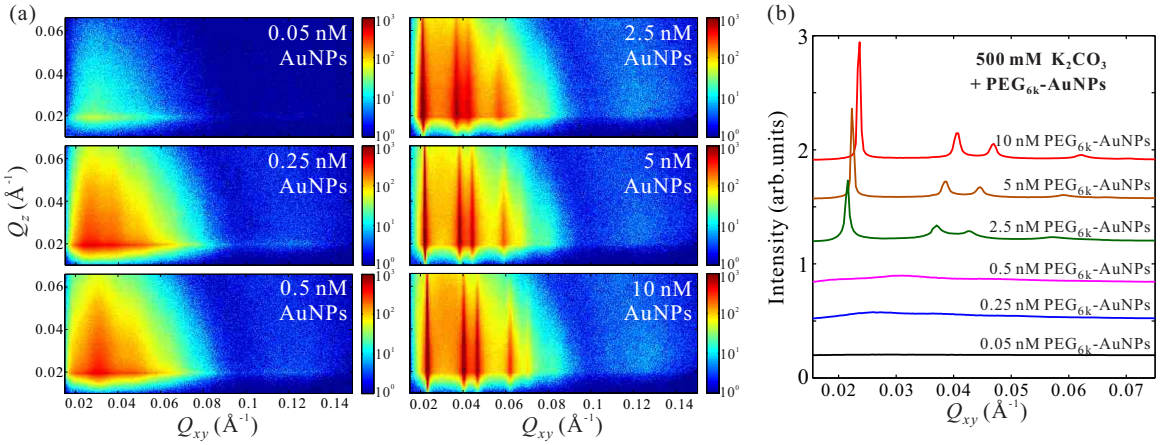

Fig. S3 (a) GISAXS patterns as functions of Q_{xy} and Q_z for aqueous solutions of PEG_{6k}-AuNPs at different nanoparticle concentrations (0.05 – 10 nM) in the presence of 0.5 M K_2CO_3. Intensities are displayed on logarithmic scales. (b) Horizontal linecut profiles along Q_{xy} direction at Q_z = 0.020 Å^{-1} integrated over Q_z range 5 $\times 10^{-3}$ Å^{-1} at low Q_{xy} range (0.02–0.07Å^{-1}) from GISAXS patterns in (a). The plots are vertically shifted for clarity.

Short chain PEG_{800}-AuNPs crystallization

In this Section, we present the evolution of the Gibbs monolayer from the gas- to liquid- to superlattice-crystallization of PEG_{800}-AuNPs both as a function of salt concentration, Fig. S4 and as a function of PEG-AuNP concentration, Fig. S5. The analysis shows that the crystallization takes place only at much higher K_2CO_3 concentrations than for PEG_{6k}-AuNPs and as expected the lattice constant scales with the length of PEG, thus the length of PEG can be used as a knob to tune the lattice constant as well.

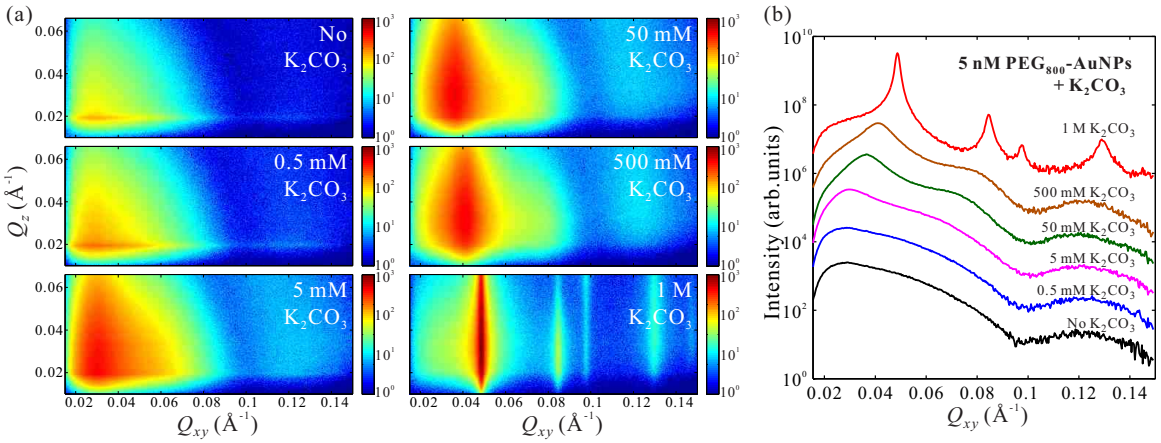

Fig. S4 (a) GISAXS patterns as functions of Q_{xy} and Q_z for aqueous solutions of 5 nM PEG_{800}-AuNPs in the absence of salts and in the presence of different concentrations of K_2CO_3 (0.5 mM – 1 M). Intensities are displayed on logarithmic scales. (b) Horizontal linecut profiles along Q_{xy} direction at Q_z = 0.020 Å^{-1} integrated over Q_z range 5 $\times 10^{-3}$ Å^{-1} at low Q_{xy} range (0.02–0.07Å^{-1}) from GISAXS patterns in (a). The plots are vertically shifted for clarity.

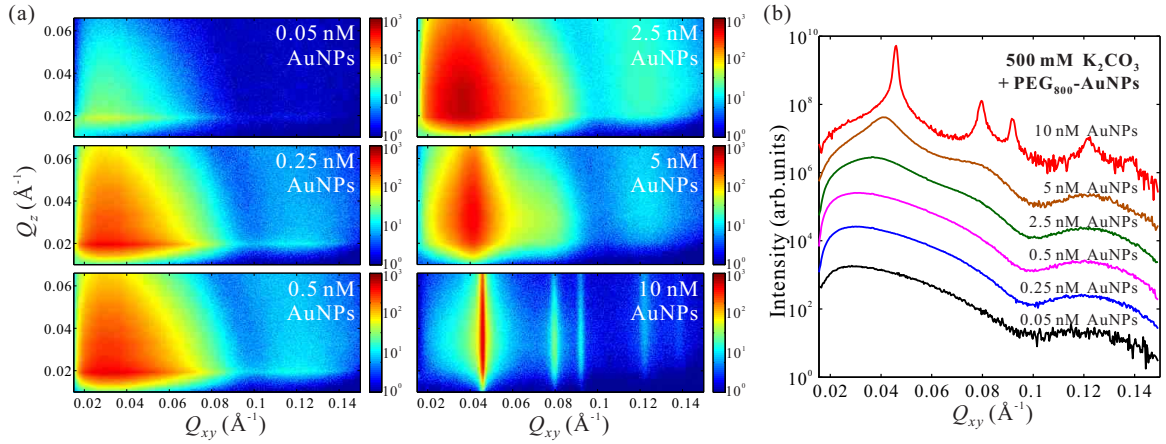

Fig. S5 (a) GISAXS patterns as functions of Q_{xy} and Q_z for aqueous solutions of PEG_{800}-AuNPs with different nanoparticle concentrations (0.05 – 10 nM) in the presence of 0.5 mM K_2CO_3. Intensities are displayed on logarithmic scales. (b) Horizontal linecut profiles along Q_{xy} direction at Q_z = 0.020 Å^{-1} integrated over Q_z range 5 $\times 10^{-3}$ Å^{-1} at low Q_{xy} range (0.02–0.07Å^{-1}) from GISAXS patterns in (a). The plots are vertically shifted for clarity.

Estimated surface coverage of crystalline PEG-AuNP superlattices

Here, we estimate the maximum in the electron density (ED) of monolayers of 2D crystalline PEG-AuNPs based on a space filling model using the known EDs of water and pure Au, and the 2D crystalline structures determined by GISAXS. We then compare our calculated maximum ED to the one obtained from the X-ray reflectivity to estimate the macroscopic surface coverage of the 2D crystalline PEG-AuNPs.

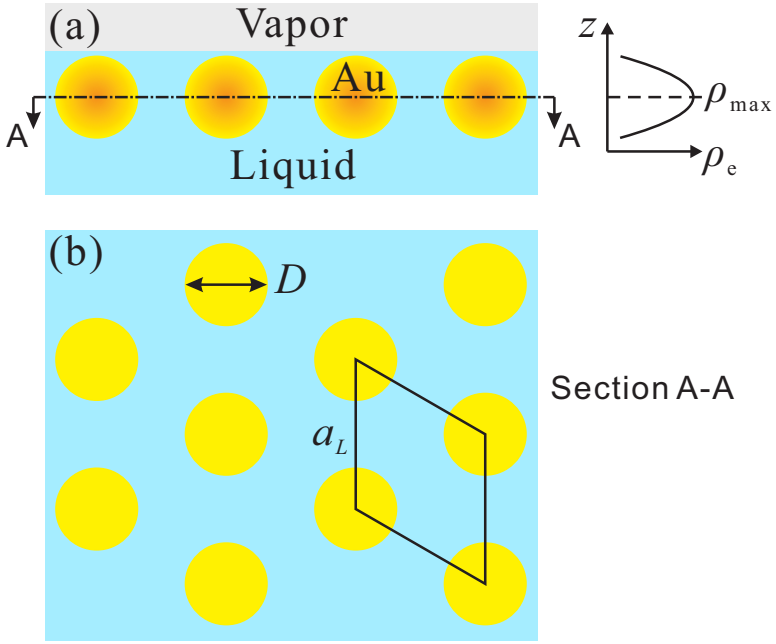

Fig. S6 A schematic of a nanoparticle monolayer at the vapor-liquid interface with corresponding ED profile along surface-normal direction, associated with the sectional view at the maximum ED position.

We assume that in the mono-particle layer of the 2D crystalline, all AuNPs are perfectly packed in the same plane, leading to a maximum ED at the plane occupied by the centers of AuNPs as illustrated in Fig. S6a. The corresponding sectional view at the maximum ED position is shown in Fig. S6b. In this maximum ED plane, the area fraction of AuNPs in the unit cell of a 2D hexagonal crystalline is $\phi = A_{\rm np}/A_{\rm 2D}$, where the area occupied by an AuNP is $A_{\rm np} = \pi D^2/4$, and the area of a 2D unit cell with a lattice constant a_L is $A_{\rm 2D} = a_L^2\sqrt{3}/2$. The ED of pure gold is $\rho_{\rm Au} = 79\rho N_A/M_{\rm Au} = 4.66$ e/Å^3, where $\rho = 19.3$ g/cm^3, $N_A = 6.02 \times 10^{23}$ mol^{-1} and $M_{\rm Au} = 196.97$ g/mol are bulk gold density, Avogadro number and atomic weight of gold, respectively. The ED of subphase area surrounding the AuNPs ($\rho_{\rm sub}$) is considered as ED of pure K_2CO_3 solution with the same concentration to the bulk (contribution of the PEG shell to the ED is the same as that of surrounding media, which is justified by our SAXS results; see Fig. S2). Assuming that K_2CO_3 solids dissolved in pure water increase the ED of aqueous solution without changing the solution volume, the ED of K_2CO_3 solution at the concentration

Table S1 Maximum electron density of 2D PEG-AuNP superlattices at the vapor-liquid interface

MW of PEG	[PEG-AuNPs] n_s (nM)	[K_2CO_3] I (M)	Lattice constant a_L (Å)	ED of K_2CO_3 solution $\rho_{K_2CO_3}$ (e/Å^3)	Estimated maximum ED ρ_{2Dmax} (e/Å^3)	Maximum ED extracted from XRR ρ_{max} (e/Å^3)	Estimated surface coverage ψ
6000	5	0.005	388 ± 4	0.3342	0.532–0.540	~0.531	≥ 96 %
6000	5	0.05	366 ± 5	0.3360	0.557–0.569	~0.557	≥ 95 %
6000	5	0.5	322 ± 3	0.3545	0.641–0.652	~0.645	≥ 98 %
6000	5	1	245 ± 2	0.3749	0.868–0.885	~0.695	≥ 63 %
6000	2.5	0.5	338 ± 4	0.3545	0.613–0.626	~0.589	≥ 87 %
6000	10	0.5	309 ± 3	0.3545	0.665–0.677	~0.617	≥ 81 %
800	5	1	149 ± 1	0.3749	1.712–1.749	~1.322	≥ 69 %
800	10	0.5	158 ± 3	0.3545	1.551–1.581	~1.783	~ 100 %

of c (in Molar) is estimated to be $\rho_{K_2CO_3} = \rho_w + 68cN_A/10^{27} = 0.334 + 0.0410c$ e/Å^3. Using the space filling model, the maximum ED of 2D crystalline structure is $\rho_{2Dmax} = \rho_{Au}\phi + \rho_{sub}(1-\phi)$. The calculated maximum ED results are summarized in Table S1 below. Overall, the estimates are close to the results measured by XRR. Applying the calculated ρ_{2Dmax} and the measured maximum ED ρ_{max} extracted from XRR, the surface coverage of 2D crystalline is $\psi = (\rho_{max} - \rho_{sub})/(\rho_{2Dmax} - \rho_{sub})$ (See Table S1). The surface coverage is nearly 100 %. We note that in this simple model the surface coverage of 2D crystalline is underestimated owing to the assumption of perfect lateral packing of AuNPs in the same plane and the negligence of surface roughness.

Hydrodynamic size of AuNPs and PEG-AuNPs in salts

Using dynamic light scattering we estimate the hydrodynamic size of bare and PEG-capped particles. Unlike polyelectrolyte-capped AuNPs (including ssDNA-AuNPs), as shown in Fig. S7, the hydrodynamic size distribution of PEG-AuNPs remains practically the same in the presence of salts. This also shows that the polymer in PEG_{800}-AuNPs is too short to behave like the theoretically infinitely long polymer brush.

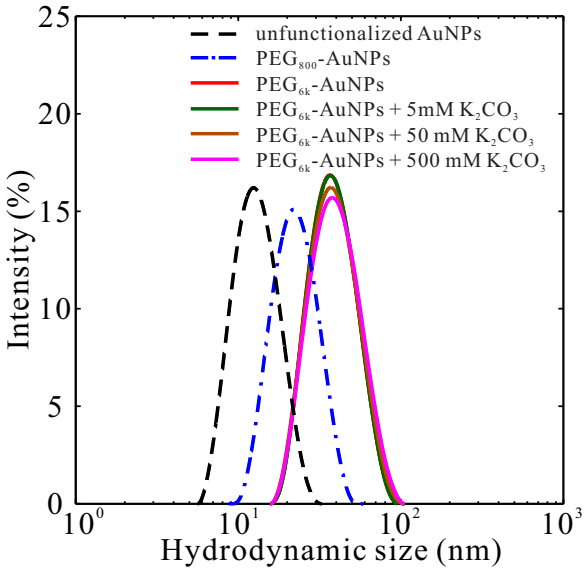

Fig. S7 Dynamic light scattering (DLS) measurements of unfunctionalized AuNPs, PEG_{800}-AuNPs and PEG_{6k}-AuNPs dispersed in the bulk solution under different conditions as indicated. The AuNPs with PEG shells clearly show larger hydrodynamic size than that of the bare Au cores (unfunctionalized AuNPs). In addition, DLS results of PEG_{6k}-AuNPs with or without K_2CO_3 indicate that the presence of K_2CO_3 in the solution (up to 0.5 M) have little effect on the hydrodynamic size of nanoparticles in the bulk.

Grafting density of PEG on AuNPs

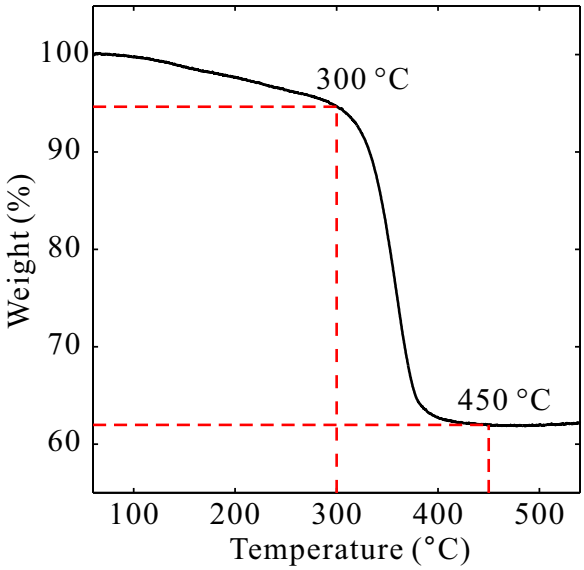

Fig. S8 Weight loss of PEG_{6k}-AuNPs as function of temperature. The weight loss between 300 °C and 450°C corresponds to the thermal degradation of the PEG.

Thermogravimetric analysis (TGA) is used to estimate the grafting density of PEG on AuNPs. The concentrated PEG-AuNPs is dried at 60 °C for 4 hours prior to TGA measurements. The TGA is carried out under a nitrogen atmosphere from 25 to 800 °C at a ramp rate of 10 °C/min. The weight loss between 300 °C and 450°C corresponds to the thermal degradation of the PEG. For instance, the weight loss of PEG_{6k}-AuNPs as function of temperature is shown in Fig. S8. The weight percentage at 300 °C and 450°C are 94.66 % and 61.96 %, respectively. Therefore, 32.70 % of weight is related to the PEG_{6k} loaded on AuNPs, and 61.96 % of weight is from pure AuNPs. The weight of each AuNP is $m_{\rm np} = \rho\pi D^3/6$, where $\rho = 19.3$ g/cm^3 is bulk gold density, $D = 8.8 \pm 0.9$ nm is the diameter of the AuNP. The molecular weight of PEG_{6k} is $m_{\rm PEG} = 6000$. Thus, the number of PEG_{6k} per AuNP is $n = (32.70 m_{\rm np})/61.96 m_{\rm PEG} = 367$. The grafting density is $\sigma = n/(\pi D^2) = 1.51$ chains/nm^2.

Theoretical Model

Physical parameters of PEG

There is a considerable range of values for the Kuhn length, Flory characteristic ratio C_n and Kuhn monomer mass M_0 in the literature. The values used here are calculated from Mark and Flory[44], who report the values for PEG (also called PEO) in salt at the θ-point, the exact conditions analyzed in this paper, as

$$\langle r^2\rangle/ml^2 = C_\infty = 4.1(0.4), \tag{S1}$$

where $\langle r^2\rangle$ is the mean square unperturbed end-to-end distance for a real chain, $l^2 = (2l_{co}^2 + l_{cc}^2)/3.0$ and $l_{co} = 1.43$ Å, $l_{cc} = 1.53$ Å are the O – C and C – C bond lengths, and $m = 3N_r$ is the number of bonds and N_r is the number of C – C – O groups in the polymer. The maximum extension of a PEO chain is therefore

$$R_{max} = (2l_{co} + l_{cc})\cos(\theta/2)N_r = 3.64N_r \ \ (\text{Å}) \ , \tag{S2}$$

where $\theta = 68^\circ$ is the bond angle, which is the same for all three atoms in the monomer. The Kuhn length is[47]

$$b = \frac{C_\infty l^2 m}{R_{max}} = 7.24 \ (\text{Å}) \tag{S3}$$

and the equivalent number of monomers of a Gaussian chain is

$$N = \frac{R_{max}^2}{C_\infty m l^2} = 0.503 N_r. \tag{S4}$$

Using that the molecular weight of a PEO monomer is $M_1 = 2M_C + M_O + 4M_H = 44.052$, it is

$$M_0 = M_1/0.503 = 87.6. \tag{S5}$$

Thus for the two PEO used in this paper, the number of independent Kuhn monomers is

$$N_{6k} = 6000/87.6 = 68.5 \ (N_r = 136) \tag{S6}$$

$$N_{800} = 800/87.6 = 9.13 \ (N_r = 18) \ . \tag{S7}$$

For the PEG_{800}, the approximation $C_n \approx C_\infty$ is certainly questionable, and explains the larger hydrodynamic radius than the theoretical estimate.

PEG-AuNPs in solution

As described in Refs.[30,31] the three component system water-salt-PEG typically separates into two phases, an all PEG solvated by liquid A and liquid B. Liquid A consists of water and a relatively low salt concentration (a few percent weight or less), and liquid B with a higher salt concentration of ten percent or more. Early efforts to predict the phase diagram of this three component system showed a limited success[50,51] as it was noted that there is a specific salt-PEG interaction, presumably through the ether oxygens and the salt cations. Therefore, we consider a model where the salt is implicit, based on the following assumptions:

- Liquid A is a θ-solvent for PEG.
- Liquid B is a poor solvent for PEG.
- When equilibrium is established, an interface between liquid A and liquid B is formed with surface tension γ_{AB}.

The first assumption is justified as liquid A is the phase boundary for PEG. The second assumption follows from the fact that no PEG is found in liquid Refs.[30,31].

We consider a PEG-AuNP as consisting of n flexible chains with N monomers covalently grafted at the surface of the nanoparticle core, whose radius is R. The grafting density is thus $\sigma = n/4\pi R^2$. We first treat PEG-AuNPs in solution and then its crystallization at the interface.

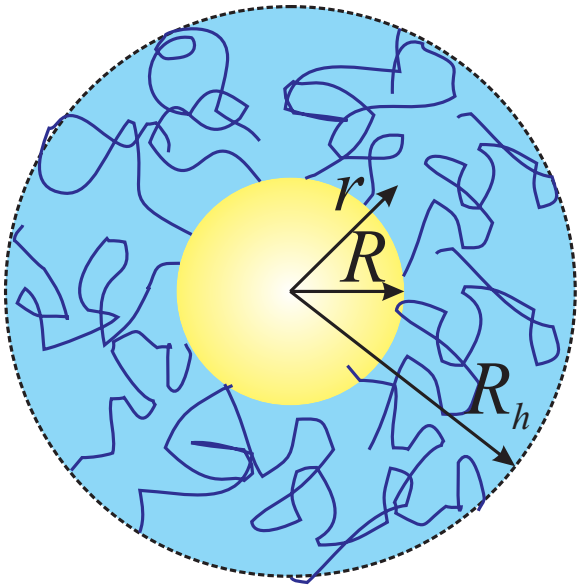

Fig. S9 Depiction of PEG-AuNP brush, and the parameters used.

Following Ref.[46], we consider PEG as gaussian chains with three-body interactions at the θ-point (first assumption). The monomer density at a distance r from the center is given (for $r > R$)

$$\phi(r) = \frac{R}{r}(\sigma b^2)^{1/2}(2w_0)^{-1/4} \ , \tag{S8}$$

where b is the Kuhn length, σ is the grafting density and w_0 is the dimensionless three-body interaction. The spherical radii R_h is obtained by imposing that the integral of the above density is equal to the total number of monomers $= Nnb^3$, leading

$$\left(\frac{R_h}{R}\right)^2 = 1 + 2\frac{N}{R/b}(\sigma b^2)^{1/2}(2w_0)^{1/4} \ . \tag{S9}$$

For future reference, we will also need the free energy for the spherical brush at the θ point. It is given as

$$\frac{f_r}{k_BT} = 4\pi\left(\frac{R}{b}\right)^3 (\sigma b^2)^{3/2}(2w_0)^{1/4}\log(1+2\frac{N}{R/b}(\sigma b^2)^{1/2}(2w_0)^{1/4}). \tag{S10}$$

To this free energy, there is an additional term that arises from the surface tension between polymer/liquid A and liquid B. We will assume that liquid B is a slightly poor solvent for PEG. This latter condition is defined by $\xi(r=R_h) < \xi_T$, where $\xi(r) = r/R\sqrt{\sigma}$ and $\xi_T = b/(2\chi-1)$ is the thermal correlation length[47], and $\chi > 1/2$ parameterizes the quality of solvent B to PEG. In the opposite limit $\xi(r=R_h) > \xi_T$, which is not discussed here, PEG would collapse into globules, and the size of the PEG-AuNPs is not described by Eq. S8. The surface tension free energy is given by

$$f_s = \gamma_{AB} 4\pi R_h^2 \, . \tag{S11}$$

Based on general arguments, we expect $\gamma_{AB} \approx k_BT(2\chi-1)^2/b^2$.

Finally, because the PEG-AuNPs are in solution, there is the ideal term

$$F_t = N_s k_BT(\log(n_s v_0) - 1) \, , \tag{S12}$$

where N_s is the number of PEG-AuNPs in solution and $n_s = N_s/V$ its number density. The chemical potential of the bulk PEG-AuNPs is given by

$$\mu_B = \frac{\partial F}{\partial N_s} = f_r + f_s + k_BT\log(n_s v_0). \tag{S13}$$

PEG-AuNPs at the interface

At the interface, the free energy of the PEG-AuNPs is modified in three ways: the brushes are compressed, the surface area of contact with solvent B is much reduced, and finally, there is a reduction of translational entropy.

The stretching energy of two compressed brushes has been authoritative reviewed in Ref.[48]. Unfortunately, no simple expression is available for the experimental conditions, and a full calculation is beyond the scope of this paper. Therefore, we opt for a more heuristic derivation, based on the modified Derjaguin approximation for the excess free energy

$$F_e(z) = 2\pi R^2(R+z)\int_z^{H_0} \frac{f(H)-f(H_0)}{(R+H)^2}dH \equiv 2\pi R^2(R+z)\int_z^{H_0}\frac{\Delta f(H)}{(R+H)^2}dH \, . \tag{S14}$$

Here, $2(R+z)$ is the center-to-center distance of the two brushes and $H_0 = R_h - R$ is the uncompressed brush height. The quantity $f(H)$ is the free energy per unit area of a uniformly compressed spherical brush at a radius $H < H_0$. It is given as

$$\Delta f(y) = \frac{R}{b}(\sigma b^2)^{3/2}(2w_0)^{1/4}\frac{1}{b^2}G(y) \tag{S15}$$

where $y = (R+z)/R_h$. Note that the function $G(x)$ satisfies that $G'(1) = 0$, $G''(1) \approx 32.6 > 0$, and the latter condition is the statement that the uncompressed brush is a minimum of the free energy. Detailed derivations for these results will be published elsewhere. The actual potential between two PEG-AuNPs is then given as

$$F_e(z) = 2\pi\left(\frac{R}{b}\right)^3 (\sigma b^2)^{3/2}(2w_0)^{1/4} y H(y) \, , \tag{S16}$$

where $H(y) = \int_y^1 \frac{dw}{w^2}G(w)$, and $G(y)$ has been defined in the previous equation. Note that $H(1) = H'(1) = H''(1) = 0$. For small compressions, $1-y << 1$, the above expression reduces to

$$F_e(z) = 2\pi\left(\frac{R}{b}\right)^3 (\sigma b^2)^{3/2}(2w_0)^{1/4}\frac{G''(1)}{6}(1-y)^3 \, . \tag{S17}$$

It should be noted, however, that the exact formula shows that the approximation Eq. S17 has a small range of applicability as the resulting potential quickly picks up significant non-harmonic contributions for $y \lesssim 0.85$.

We assume that the surface in contact with solvent B is the area of the plane occupied by the PEG-AuNPs at the interface. The free energy of a single nanoparticle is given as

$$F_s(z) = \gamma_{AB} 2\sqrt{3}(R+z)^2 \, . \tag{S18}$$

Finally, the entropic term is given, within dynamic lattice theory (DLT)[49].

$$F_d(z) = k_BT(g(R_h) + \log(v_0)) \, , \tag{S19}$$

where $g(z) = \frac{1}{2N_i}\log\left[\det(\frac{D_{ij}}{2\pi k_BT})\right]$, where N_i is the number of particles at the interface and D_{ij} is the dynamical matrix. Although it is possible to calculate the above determinant exactly for an hexagonal two dimensional lattice, the formula is excessively complex. We

therefore make the free volume approximation

$$F_d(z) = k_B T \log(v_0/(4\pi y^2 R_h^3/3)) \ . \tag{S20}$$

The chemical potential of the PEG-Au at the interface is given by

$$\mu_I = F_s(z) + qF_e(z) + F_r + k_B T \log(v_0/(4\pi y^2 R_h^3/3)) \ . \tag{S21}$$

Equilibrium condition

The condition of equilibrium between bulk and interface leads to the equation

$$\mu_I = \mu_B \ , \tag{S22}$$

or, in explicit form:

$$\begin{aligned}(4\pi - 2\sqrt{3})\frac{\gamma_{AB}}{k_B T} R_h^2 + \log(n_s 4\pi R_h^3/3) \quad &= \quad -2\sqrt{3}\frac{\gamma_{AB}}{k_B T} R_h^2 (1-y^2) + \\ &+ \quad 2\pi \left(\frac{R}{b}\right)^3 (\sigma b^2)^{3/2} (2w_0)^{1/4} y H(y) - \log(y^2) \ ,\end{aligned} \tag{S23}$$

which determines y, and from it, the lattice constant a_L from $y = \frac{2R_h - a_L}{2R_h}$, as a function of the physical parameters. The above equations illustrate a physical mechanism where the dramatic reduction in surface tension that occurs when particles reach the interface entirely drives the crystallization process.

For the purposes of illustrating the physical mechanism, one can assume that the reduction of surface tension is opposed by the stretching or compression energy, and that the small compression limit Eq. S17 can be applied. With these approximations, it follows:

$$(1 - \frac{a_L}{2R_h})^3 = (4 - \frac{2\sqrt{3}}{\pi})\frac{1}{\sigma b^2}\left(\frac{b}{R}\right)^2 \frac{6N}{qG''(1)}\left(\frac{\gamma_{AB} b^2}{k_B T} + \frac{b/R \log(n_s v_l)}{(8\pi - 4\sqrt{3})N(\sigma b^2)^{1/2}(2w_0)^{1/4}}\right) \ , \tag{S24}$$

where $v_l = \frac{4\pi}{3} R_h^3$.

Quality of the solvent

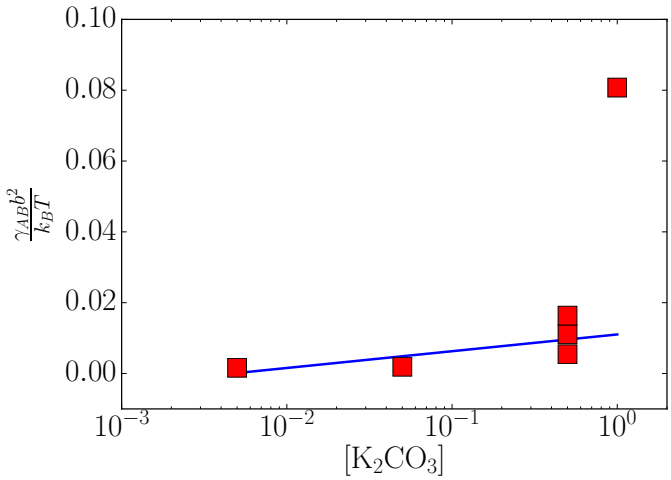

Fig. S10 Fit of the solvent quality as described below. The results are for PEG_{6k}-AuNPs. Clearly, the last point, corresponding to 1 M K_2CO_3 concentration, is not consistent with a simple logarithmic dependence

From the reported values of $\frac{2R_h - a_L}{2R_h}$ (Table S1), and the assumption that the solvent quality parameter is described by the two parameter formula

$$\gamma_{AB} b^2/k_B T = \tau log(I/I_0) \tag{S25}$$

a fit is performed, with $I_0 = 0.0046$ M and $\tau = 0.0021$. Here I is the K_2CO_3 concentration, $[K_2CO_3]$. Although the quality of the fit is adequate up to about 0.5 M, it illustrates that the data is consistent with a moderately poor solvent, not far from ideal. The point at the higher salt concentration illustrates that the surface tension grows more rapidly than the logarithmic fit Eq. S25 at high ionic strengths consistent with the onset of precipitates into 3D solids.